

# On Optimization of Traffic Flow Performance for Conservation Laws on Networks

**Fabio Ancona**

*Dip. di Matematica “Tullio Levi-Civita”, Università di Padova, 35121 Padova, Italy  
ancona@math.unipd.it*

**Annalisa Cesaroni**

*Dipartimento di Scienze Statistiche, Università di Padova, 35121 Padova, Italy  
annalisa.cesaroni@unipd.it*

**Giuseppe Maria Coclite**

*Dip. di Meccanica, Matematica e Management, Politecnico di Bari, 70125 Bari, Italy  
giuseppemaria.coclite@poliba.it*

**Mauro Garavello**

*Dip. di Matematica e Applicazioni, Università di Milano Bicocca, 20125 Milano, Italy  
mauro.garavello@unimib.it*

Received: July 17, 2019

Accepted: September 16, 2019

We investigate several optimization problems related to different traffic performance indexes considered in the literature: to diminish mean travel time or queue lengths, to minimise stop-and-go waves, or to get a fuel consumption reduction. We analyze these problems within the general control setup for conservation law models on networks recently proposed by the authors [*On the optimization of conservation law models at a junction with inflow and flow distribution controls*, SIAM J. Control Optimization 56 (2018) 3370–3403]. The existence of optimal solutions for the above mentioned problems is obtained in the context of distribution and inflow controls acting at a single junction. A variational formulation of such optimization problems is also provided and some numerical simulations of optimal solutions are discussed.

*Keywords:* Conservation laws, traffic models, networks, weak solutions.

*2010 Mathematics Subject Classification:* 35F25, 35L65, 90B20.

## 1. Introduction

In the last two decades there have been great strides in the modelling and analysis of optimal control problems for hyperbolic conservation laws evolving on networks (see the monographs [9, 23] and references therein). The raising interest in such problems is motivated by a wide range of applications in different areas, such as data flow and telecommunication [13], gas or water pipeline [18, 27], production processes [20, 21, 26, 34], evacuation models [25], biological resources [15], and blood circulation [11]. In the aforementioned models, networks are directed graphs on

The authors are members of the Gruppo Nazionale per l’Analisi Matematica, la Probabilità e le loro Applicazioni (GNAMPA) of the Istituto Nazionale di Alta Matematica (INdAM). The authors were partially supported by the Istituto Nazionale di Alta Matematica “F. Severi”, through GNAMPA and by PRAT 2013- Traffic Flow on Networks: Analysis and Control, University of Padova.

which the flow of some quantity evolves in time along its edges (or arcs) connected by the vertices (or nodes, or junctions) of the graph. One assumes that on each arc it is separately satisfied a conservation law describing the evolution of the unknown density, and that suitably coupling conditions hold true at the junctions. A minimal requirement is that, at the nodes, a Kirchoff type condition is verified so to guarantee the conservation of the total mass. Typically, in order to achieve well-posedness of the Cauchy problem, this condition is supplemented with some flow distribution rules of the incoming flux-densities with respect to the outgoing ones, and with an entropy-type condition to timewise maximize the total flux through the junction. In particular, the resulting solution is usually characterized in terms of a junction Riemann solver. Such a solver prescribes a rule to construct a unique self-similar solution of a Cauchy problem with constant initial data on each incoming and outgoing edge of the junction (see [24]).

A different perspective was introduced in [3] to analyze control problems for conservation law models on networks. Namely, the flow distribution parameters and the incoming fluxes at a junction (that are compatible with the corresponding distribution rules) are treated as controls which determine a unique solution of the Cauchy problem. In this framework, an admissible solution of the Cauchy problem may exhibit at the junctions rarefaction waves originated at positive times or stationary nonclassical shocks (see [37]) which are instead precluded in the classical setting based on the introduction of appropriate junction Riemann solvers. Because of the finite speed of propagation of hyperbolic models, it is sufficient to analyze these problems in a neighbourhood of each node of the network to capture the fundamental properties of solutions of interest herein.

The aim of this paper is to investigate traffic flow performance for conservation law models on networks within the control setup proposed in [3]. Starting from the seminal papers by Lighthill, Whitham and Richards (LWR model) [39, 44], fluid-dynamic models describing unidirectional car traffic as a continuum (where the dynamical variable is the traffic density) have been intensively discussed in recent years. We refer for example to [10, 14, 29, 31, 35] for network models of vehicular traffic based on conservation laws.

Efficient traffic flow management is an object of increasing attention by road planners and traffic controllers to mitigate traffic congestion, accidents and pollution, which have huge economic impact, beside affecting people's quality of life. We shall thus consider here some optimization problems related to different traffic performance indexes introduced in the literature to improve the mean travel time in a given road segment [5, 6, 12, 42, 50], to diminish the queue length due to a red light or stop sign [19], to minimise stop-and-go waves [16, 17, 28, 48], or to get a fuel consumption reduction [4, 43].

From a practical point of view, traffic control can be implemented in a variety of ways, which includes the use of route information panels giving recommendations to the drivers to take one of the outgoing roads, the use of ramp meter signals, traffic light timing, yielding and stop signs, integrated vehicular and roadside sensors so to modulate the amount of incoming fluxes entering the junction.

We will show existence of optimal solutions for the above mentioned problems formulated in the context of controls acting at a single junction, and we will provide an

equivalent variational formulation of the optimization problems herein considered. We shall also investigate numerically the behaviour of some optimal solutions.

## 2. The junction Cauchy problem for conservation laws

As in [3], we consider a directed graph composed by a single node, located at  $x = 0$ , with  $m$  incoming arcs  $I_i = (-\infty, 0)$ ,  $i \in \mathcal{I} = \{1, \dots, m\}$ , and  $n$  outgoing ones  $I_j = (0, +\infty)$ ,  $j \in \mathcal{O} = \{m + 1, \dots, m + n\}$ . On each arc  $I_\ell$ , the evolution of the unknown density  $u_\ell(t, x)$  is governed by a scalar conservation law

$$\partial_t u_\ell + \partial_x f_\ell(u_\ell) = 0, \quad t \geq 0, \quad x \in I_\ell. \tag{1}$$

The flux function  $f_\ell : \Omega_\ell \rightarrow \mathbb{R}$  is defined on a compact interval  $\Omega_\ell = [0, u_\ell^{max}]$ , where  $u_\ell^{max}$  denotes the maximum possible density (bump-to-bump) inside the road  $I_\ell$ . In particular, we assume that the fundamental diagram  $f_\ell$  satisfies the following assumptions:

- (A) (1)  $f_\ell(u) = uv_\ell(u)$  where  $v_\ell \in \mathbf{C}^1(\Omega_\ell; \mathbb{R})$  is the speed, and we assume that  $v_\ell(u^{max}) = 0$ ;
- (2)  $f$  is strictly concave and  $f'_\ell(u_\ell^{max}) < 0 < f'_\ell(0)$ .

We denote by  $\theta_\ell \in \Omega$  the unique point of global maximum for  $f_\ell$ , i.e.

$$\theta_\ell \doteq \arg \max_{u \in \Omega_\ell} f_\ell(u),$$

and, for every  $u \in \Omega_\ell \setminus \{\theta_\ell\}$ , we denote by  $\pi_\ell(u)$  the unique point in  $\Omega_\ell$  such that

$$f_\ell(u) = f_\ell(\pi_\ell(u)) \quad \text{and} \quad \pi_\ell(u) \neq u,$$

while we set  $\pi_\ell(\theta_\ell) \doteq \theta_\ell$ . In order to reduce the queue formation at the junction, we make the assumption that the total capacity of the outgoing roads is larger than the incoming ones, i.e.

$$\sum_{i \in \mathcal{I}} f_i(\theta_i) \leq \sum_{j \in \mathcal{O}} f_j(\theta_j). \tag{2}$$

**Remark 2.1.** For traffic flow applications, the maximum density  $u_\ell^{max}$  is only related on the length of cars and does not depend on the roads of the network. Similarly the speed of cars  $v_\ell$  is expected to be a decreasing function of the density.

However we prefer to consider in this paper slightly more general cases, including the possibility to have different maximum densities on different arcs of the network and that  $v_\ell$  is not necessary a decreasing function. From a mathematical point of view, this is not an issue whenever the flux function satisfies the assumption (A). Moreover this choice leaves open the possibility of using this model in different contexts and applications. □

The notion of solution of the Cauchy problem for such a node is given in terms of solutions to  $m+n$  Dirichlet boundary value problems coupled with distribution transition conditions. Thus, given an  $(m+n)$ -tuple of initial data  $\bar{u} \in \prod_{\ell=1}^{m+n} \mathbf{L}^\infty(I_\ell; \Omega_\ell)$  and boundary data  $k \in \prod_{\ell=1}^{m+n} \mathbf{L}^\infty([0, +\infty); \Omega_\ell)$ , consider, for every  $i = 1, \dots, m$ ,  $j = m + 1, \dots, m + n$ , the mixed initial-boundary value problems

$$\begin{cases} \partial_t u_i + \partial_x f_i(u_i) = 0 & x < 0, t > 0, \\ u_i(0, x) = \bar{u}_i(x) & x < 0, \\ u_i(t, 0) = k_i(t) & t > 0, \end{cases} \tag{3}$$

$$\begin{cases} \partial_t u_j + \partial_x f_j(u_j) = 0 & x > 0, t > 0, \\ u_j(0, x) = \bar{u}_j(x) & x > 0, \\ u_j(t, 0) = k_j(t) & t > 0. \end{cases} \tag{4}$$

Here, and throughout the following, we adopt the notation  $u_\ell(t, 0)$  for the one-sided limit  $u_\ell(t, 0^\pm) \doteq \lim_{x \rightarrow 0^\pm} u_\ell(t, x)$  of  $u_\ell(t, \cdot)$  at the boundary  $x = 0$ . We recall, see [3, Remark 2.3], that an entropy admissible weak solution  $u_\ell(t)$  of (1) satisfies a-priori BV-bounds at any fixed time  $t > 0$  and that, for every  $\ell \in \mathcal{I}$  ( $\ell \in \mathcal{O}$ ),  $u_\ell(t)$  admits the one-sided limit  $u_\ell(t, 0^-)$  ( $u_\ell(t, 0^+)$ ). Moreover, for every fixed point  $x \in I_\ell$ ,  $\ell \in \mathcal{I} \cup \mathcal{O}$ , one has  $f_\ell(u_\ell(\cdot, x)) \in \mathbf{BV}_{\text{loc}}((0, +\infty); f_\ell(\Omega_\ell))$ . The Dirichlet conditions in (3), (4) are interpreted in the relaxed sense of Bardos, Le Roux, Nédélec [7] which, for strictly concave fluxes, are equivalent to the condition (iii) stated in the definition below of entropy admissible solution of the mixed initial-boundary value problem (cfr. [36]).

**Definition 2.2.** Given  $\bar{u}_\ell \in \mathbf{L}^\infty(I_\ell; \Omega_\ell)$  and  $k_\ell \in \mathbf{L}^\infty([0, +\infty); \Omega_\ell)$ ,  $\ell \in \mathcal{I} \cup \mathcal{O}$ , we say that a function  $u_\ell \in \mathbf{C}([0, +\infty); \mathbf{L}^1_{\text{loc}}(I_\ell; \Omega_\ell))$  is an *entropy admissible weak solution* of (3) (resp. of (4)) if:

- (i) For every  $t > 0$ ,  $u_\ell(t) \in \mathbf{BV}_{\text{loc}}(I_\ell; \Omega_\ell)$  and admits the one-sided limit at  $x = 0$ .
- (ii)  $u_\ell$  is a weak entropic solution of (1) with initial data  $\bar{u}_\ell$ , i.e., we have for all  $\varphi \in \mathcal{C}^1_c(\mathbb{R} \times I_\ell; \mathbb{R})$

$$\int_0^{+\infty} \int_{I_\ell} [u_\ell \partial_t \varphi + f_\ell(u_\ell) \partial_x \varphi](t, x) \, dx dt + \int_{I_\ell} \bar{u}_\ell(x) \varphi(0, x) dx = 0,$$

and the Lax entropy condition is satisfied:

$$u_\ell(t, x^-) \leq u_\ell(t, x^+) \quad t > 0, x \in I_\ell \setminus \{0\}.$$

- (iii) The boundary condition in (3) is verified if, for a.e.  $t > 0$ , there holds:

$$\begin{aligned} \text{either} & \quad u_i(t, 0) = \max\{k_i(t), \theta_i\} \\ \text{or} & \quad f'_i(u_i(t, 0)) > 0 \quad \text{and} \quad f_i(u_i(t, 0)) \leq f_i(\max\{k_i(t), \theta_i\}); \end{aligned} \tag{5}$$

the boundary condition in (4) is verified if, for a.e.  $t > 0$ , there holds:

$$\begin{aligned} \text{either} & \quad u_j(t, 0) = \min\{k_j(t), \theta_j\} \\ \text{or} & \quad f'_j(u_j(t, 0)) < 0 \quad \text{and} \quad f_j(u_j(t, 0)) \leq f_j(\min\{k_j(t), \theta_j\}). \end{aligned}$$

**Remark 2.3.** Existence and uniqueness of entropy admissible weak solutions to the Dirichlet boundary value problems (3), (4) rely on the results in [40, 41]. We also recall the  $\mathbf{L}^1$ -contraction property enjoyed by such solutions (see [5, 36]) which we state here for the boundary value problem (4).

Given  $\bar{u}_j, \bar{u}'_j \in \mathbf{L}^\infty((0, +\infty); \Omega_j)$  and  $k_j, k'_j \in \mathbf{L}^\infty([0, +\infty); \Omega_\ell)$ ,  $j \in \mathcal{O}$ , letting  $u_j, u'_j \in \mathbf{C}([0, +\infty); \mathbf{L}^1_{\text{loc}}((0, +\infty); \Omega_j))$  denote the corresponding entropy admissible weak solutions of (4), we have for all  $t > 0$

$$\|u_j(t, \cdot) - u'_j(t, \cdot)\|_{\mathbf{L}^1(0, +\infty)} \leq \|\bar{u}_j - \bar{u}'_j\|_{\mathbf{L}^1(0, +\infty)} + \|f_j(u_j(\cdot, 0)) - f_j(u'_j(\cdot, 0))\|_{\mathbf{L}^1(0, t)}. \quad \square$$

For later use we define, for every  $i \in \mathcal{I}$  and  $T > 0$ , the constant

$$\bar{c}_i^T \doteq \int_0^T f_i(u_i(t, 0)) dt, \tag{6}$$

where  $u_i$  is the solution to (3) with the boundary datum  $k_i$  constantly equal to 0. Note that  $\bar{c}_i$  can be equivalently defined by (6) interpreting  $u_i$  as the solution to (3) with any boundary datum  $k_i$  taking values in the interval  $[0, \theta_i]$ . In fact, by (5), every such a choice of  $k_i$  yields the same solution to (3). The constant  $\bar{c}_i$  represents the total amount of vehicles present in  $I_i$  which reach the junction at  $x = 0$  within time  $T > 0$ .

The transition conditions at a junction, in a realistic car traffic model, are determined by drivers' turning preferences. As described in [14, 24, 31], the nodal condition can be thus expressed requiring that the flux traces of the solutions to (3)-(4) at  $x = 0$  satisfy some, possibly time-varying, distribution rules. Namely, we consider a  $n \times m$  Markov matrix  $A(t) = (a_{ji}(t))_{j,i}$ , with

$$0 \leq a_{ji}(t) \leq 1 \quad \forall j \in \mathcal{O}, i \in \mathcal{I}, t > 0, \quad \sum_{j=m+1}^{m+n} a_{ji}(t) = 1 \quad \forall i \in \mathcal{I}, t > 0, \tag{7}$$

and we require that, for almost every  $t > 0$ , there holds

$$f_j(u_j(t, 0)) = \sum_{i=1}^m a_{ji}(t) f_i(u_i(t, 0)). \tag{8}$$

Here  $a_{ji}(t)$  represents the fraction of drivers arriving from the  $i$ -th incoming road that wish to turn on the  $j$ -th outgoing road at time  $t$ . Notice that, because of (7), the condition (8) in particular implies a Kirchhoff type formula

$$\sum_{j=m+1}^{m+n} f_j(u_j(t, 0)) = \sum_{i=1}^m f_i(u_i(t, 0)) \quad \text{for a.e. } t > 0,$$

which expresses the conservation of the total mass through the node.

As in [3], we then introduce the following concept of solution to the Cauchy problem for a node of a network.

**Definition 2.4.** Let  $T > 0$  and  $A(\cdot) = (a_{ji}(\cdot))_{j,i} \in \mathbf{L}^1([0, T]; \mathbb{R}^{m \times n})$  be a matrix valued maps satisfying (7). Given  $\bar{u} \in \prod_{\ell=1}^{m+n} \mathbf{L}^\infty(I_\ell; \Omega_\ell)$ , we say that an *entropy admissible weak solution* to the nodal Cauchy problem (3)-(4) on  $[0, T]$ , is a function  $u \in \mathbf{C}([0, T]; \prod_{\ell=1}^{m+n} \mathbf{L}^1_{\text{loc}}(I_\ell; \Omega_\ell))$  that, for some  $k \in \prod_{\ell=1}^{m+n} \mathbf{L}^\infty([0, T]; \Omega_\ell)$ , enjoys the following properties:

- (1) for every  $i = 1, \dots, m$ , the  $i$ -th component  $u_i$  of  $u$  is an entropy admissible weak solution of (3) on  $[0, T] \times I_i$ , in the sense of Definition 2.2;

- (2) for every  $j = m + 1, \dots, m + n$ , the  $j$ -th component  $u_j$  of  $u$  is an entropy admissible weak solution of (4) on  $[0, T] \times I_j$ , in the sense of Definition 2.2;
- (3) for a.e.  $t \in (0, T]$  condition (8) is satisfied.

### 3. The control framework

We briefly review here the control framework developed in [3], to which we refer for more details and proofs, and we introduce an additional constraint for the flux at the node. Fix  $T > 0$  and  $0 < K \leq 1$ . Given  $\bar{u} \in \Pi_{\ell=1}^{m+n} \mathbf{L}^\infty(I_\ell; \Omega_\ell)$ , for every  $i \in \mathcal{I}$  and  $j \in \mathcal{O}$ , recalling Definition 2.2, consider the sets

$$\mathbb{F}_i \doteq \mathbb{F}_i(\bar{u}_i) \doteq \left\{ f_i(u_i(\cdot, 0)) \mid \begin{array}{l} u_i \text{ is a weak entropy admissible solution of (3) on} \\ [0, T] \times I_i \text{ with boundary data } k_i \in \mathbf{L}^\infty([0, T]; \Omega) \end{array} \right\}$$

$$\mathbb{F}_j \doteq \mathbb{F}_j(\bar{u}_j) \doteq \left\{ f_j(u_j(\cdot, 0)) \mid \begin{array}{l} u_j \text{ is a weak entropy admissible solution of (4) on} \\ [0, T] \times I_j \text{ with boundary data } k_j \in \mathbf{L}^\infty([0, T]; \Omega) \end{array} \right\},$$

that consists of the boundary flux-traces of all possible entropy admissible weak solutions to (3) and to (4) with initial data  $\bar{u}_i, \bar{u}_j$ , respectively. Then, we define the set of admissible matrix valued maps as

$$\mathcal{A} \doteq \left\{ A = (a_{ji}(\cdot))_{j,i} \in \mathbf{BV}([0, T]; [0, 1]^{m \times n}) \mid (7) \text{ holds for a.e. } t \in [0, T] \right\}. \quad (9)$$

We may uniquely identify every admissible solution of the nodal Cauchy Problem (3)–(4) by assigning the matrix valued map  $A \in \mathcal{A}$  and the  $m$ -tuple of boundary incoming flux-traces  $\gamma = (f_1(u_1(\cdot, 0)), \dots, f_m(u_m(\cdot, 0)))$  which, in turn, by (8) determines also  $(f_{m+1}(u_{m+1}(\cdot, 0)), \dots, f_{m+n}(u_{m+n}(\cdot, 0)))$ , the  $n$ -tuple of boundary outgoing flux-traces. We then regard  $(\gamma, A)$  as a pair of *junction controls* and we shall adopt the following definition.

**Definition 3.1.** Given  $\bar{u} \in \Pi_{\ell=1}^{m+n} \mathbf{L}^\infty(I_\ell; \Omega_\ell)$  and  $A = (a_{ji}(\cdot))_{j,i} \in \mathcal{A}$ , we say that

$$\gamma = (\gamma_1, \dots, \gamma_m) \in \Pi_{\ell=1}^m \mathbf{L}^1([0, T]; f(\Omega_\ell))$$

is an  $m$ -tuple of  $A$ -admissible boundary inflow controls if there exists a boundary datum  $k \in \Pi_{\ell=1}^{m+n} \mathbf{L}^\infty([0, T]; \Omega_\ell)$  such that the entropy admissible weak solutions  $u_i, i \in \mathcal{I}$ , and  $u_j, j \in \mathcal{J}$ , of (3) and of (4), respectively, satisfy:

1.  $f_\ell(u_\ell(\cdot, 0)) \in \mathcal{F}_\ell$  for every  $\ell \in \mathcal{I} \cup \mathcal{O}$ ;
2.  $\gamma_i(t) = f_i(u_i(t, 0))$ , for a.e.  $t \in [0, T]$  and all  $i \in \mathcal{I}$ ;
3.  $\sum_{i=1}^m a_{ji}(t) \gamma_i(t) = f_j(u_j(t, 0))$ , for a.e.  $t \in [0, T]$  and all  $j \in \mathcal{O}$ .

We denote by  $u(t, x; A, \gamma)$  the entropy admissible weak solution of (3)–(4) determined by  $\gamma$  and  $A$ . The components  $u_\ell(t, x; A, \gamma), \ell \in \mathcal{I} \cup \mathcal{O}$ , are entropy admissible weak solution of (3), (4), with normalized boundary data  $k \in \Pi_{\ell=1}^{m+n} \mathbf{L}^\infty([0, T]; \Omega_\ell)$  defined by

$$k_\ell(t) \doteq \begin{cases} f_{\ell,+}^{-1}(\gamma_\ell(t)) & \text{if } \ell \in \mathcal{I}, \\ f_{\ell,-}^{-1}(f_\ell(u_\ell(t, 0))) & \text{if } \ell \in \mathcal{O}, \end{cases}$$

where we denote as  $f_{\ell,-}, f_{\ell,+}$  the restrictions of  $f_\ell$  to the intervals  $[0, \theta_\ell]$  and  $[\theta_\ell, u_\ell^{max}]$ , respectively. □

We then define the sets of admissible junction controls as

$$\begin{aligned} \mathcal{U} &\doteq \mathcal{U}(\bar{u}) \doteq \left\{ (A, \gamma) \in \mathcal{A} \times \mathbf{L}^1([0, T]; \mathbb{R}^m) \mid \begin{array}{l} \gamma \text{ is an } m\text{-tuple of } A\text{-admissible} \\ \text{boundary inflow controls} \end{array} \right\}, \\ \mathcal{U}^M &\doteq \mathcal{U}^M(\bar{u}) \doteq \left\{ ((a_{ji})_{j,i}, \gamma) \in \mathcal{U}(\bar{u}) \mid \begin{array}{l} \text{TV}\{\gamma_i\} \leq M \ \forall i \in \mathcal{I} \\ \text{TV}\{a_{ji}\} \leq M \ \forall i \in \mathcal{I}, \forall j \in \mathcal{O} \end{array} \right\}, \quad (10) \\ \mathcal{U}_K^M &\doteq \mathcal{U}_K^M(\bar{u}) \doteq \left\{ ((a_{ji})_{j,i}, \gamma) \in \mathcal{U}^M(\bar{u}) \mid \sum_{i \in \mathcal{I}} \int_0^T \gamma_i(s) ds \geq K \sum_{i \in \mathcal{I}} \bar{c}_i^T \right\}, \end{aligned}$$

for all  $M > 0$ ,  $0 < K \leq 1$ , where the constants  $\bar{c}_i^T$  are defined in (6). Here and throughout the paper, for a function of bounded variation  $\psi \in \mathbf{BV}([\tau', \tau''])$  we define  $\text{TV}\{\psi\}$  as the *essential variation* of  $\psi$  on the open interval  $(\tau', \tau'')$  which coincides with the *pointwise variation* on  $(\tau', \tau'')$  of the right continuous or left continuous representative of  $\psi$  (see [2, Section 3.2]). For a function  $\psi \in \mathbf{BV}([0, T])$ , and a subinterval  $(\tau', \tau'') \subset [0, T]$ , we shall also denote as

$$\text{TV}_{(\tau', \tau'')}\{\psi\} \doteq \text{TV}\{\psi|_{(\tau', \tau'')}\}$$

the pointwise variation of the restriction on  $(\tau', \tau'')$  of the right continuous (or left continuous) representative of  $\psi$ .

**Remark 3.2.** One can easily verify that the sets of admissible controls  $\mathcal{U}^M$  defined by (10) are nonempty, see [3]. Moreover the sets  $\mathcal{U}_K^M$  are closed subsets of  $\mathcal{U}^M$  with respect to the  $\mathbf{L}^1$ -topology. Finally, by definition of  $\bar{c}_i^T$  and because of (2), if  $\bar{u}_j(x) \in [0, \theta_j]$  for every  $j \in \mathcal{O}$  and a.e.  $x \geq 0$ , then  $\mathcal{U}_K^M$  is non empty for every  $M > 0$ .  $\square$

**Theorem 3.3.** Fix  $\bar{u} \in \Pi_{\ell=1}^{m+n} \mathbf{L}^\infty(I_\ell; \Omega_\ell)$ . Then, for every  $M > 0$ ,  $0 < K \leq 1$ , the sets  $\mathcal{U}^M$  and  $\mathcal{U}_K^M$  in (10) are compact subsets of  $\mathbf{L}^1([0, T]; \mathbb{R}^{m \times n} \times \mathbb{R}^m)$ .

**Remark 3.4.** The admissible junction control set  $\mathcal{U}_K^M$  in (10) has been introduced in order to consider minimization problems on the junction having non trivial solutions. More precisely, the functionals proposed in Section 4 have minima when the outgoing roads are empty. This implies that a minimization on the set  $\mathcal{U}^M$  results in the trivial solution where no car passes through the junction. Instead the set  $\mathcal{U}_K^M$  poses an additional constraint on the minimum number of cars, which are obliged to pass through the junction within time  $T$ .  $\square$

#### 4. Traffic performance indexes

We consider here various traffic performance indexes introduced in the literature [5, 17, 19, 43, 50] to minimize: the average travel time, the queue length due to traffic lights, stop signs or bottlenecks, the stop-and-go wave phenomena or the overall fuel consumption. We shall adopt the perspective of a planning strategy that has to be implemented at a junction over a substantial period of time, for controlling the traffic-flow in given segments of the outgoing roads. Thus, throughout this section, we fix an initial data  $\bar{u} \in \Pi_{\ell=1}^{m+n} \mathbf{L}^\infty(I_\ell; \Omega_\ell)$ , a time  $T > 0$  and an  $n$ -tuple of locations

$\bar{x} = (\bar{x}_{m+1}, \dots, \bar{x}_{m+n})$ , with  $\bar{x}_j > 0$ ,  $j \in \mathcal{O}$ , and we consider the set of admissible junction controls  $\mathcal{U} = \mathcal{U}(\bar{u})$  in (10). Then, we define the following cost functionals related to the above mentioned minimization problems.

**Average travel time.** Various travel time definitions can be found in transport engineering literature. For microscopic models the individual travel time can be directly determined by the trajectory duration of the single vehicle. Instead, for macroscopic models as the LWR PDE, one can consider the instantaneous travel time of hypothetical vehicles travelling at a speed identical to that of the fundamental diagram, which depends on the local density. Hence, following [42, 50], we define the travel time as an average of the reciprocal of traffic speed on spatio-temporal regions. Then, for every  $(A, \gamma) \in \mathcal{U}$ , we define the average travel time to reach the locations  $\bar{x}_j$  on the outgoing arc  $I_j$ ,  $j \in \mathcal{O}$ , starting from the junction located at  $x = 0$ , as

$$\mathcal{T}_{T, \bar{x}}(A, \gamma; \bar{u}) \doteq \frac{1}{T} \sum_{j \in \mathcal{O}} \int_0^T \int_0^{\bar{x}_j} \frac{1}{v_j(u_j(t, x; A, \gamma))} dx dt, \quad (11)$$

where  $v_j$  is the speed of Assumption (A) in Section 2.

**Mean arrival time.** An alternative definition of travel time for LWR models is expressed as a weighted mean in terms of the inflows and outflows in the considered road sections. Namely, assume that the initial car density is low in the outgoing roads, say  $\bar{u}_\ell(x) \in [0, \bar{\theta}_j]$ ,  $0 < \bar{\theta}_j < \theta_j$ , for almost every  $x \in I_j$ ,  $j \in \mathcal{O}$ . Then, for sufficiently large  $T$ , and for any given  $(A, \gamma) \in \mathcal{U}$ , there will be an  $m$ -tuple  $(\tau_1, \dots, \tau_m) \in [0, T]^M$  such that

$$\int_0^T f_j(u_j(t, \bar{x}_j; A, \gamma)) dt = \int_0^{\tau_j} \sum_{i \in \mathcal{I}} a_{ji}(t) \gamma_i(t) dt + \int_0^{\bar{x}_j} \bar{u}_j(x) dx \quad \forall j \in \mathcal{O}. \quad (12)$$

This means that all vehicles in the outgoing road  $I_j$  reaching the location  $\bar{x}_j$  within time  $T$  are either vehicles present in  $I_j$  at the initial time  $t = 0$ , or are vehicles entering in  $I_j$  from the junction within time  $\tau_j$ . Hence, following [5, 6], for every  $(A, \gamma) \in \mathcal{U}$ , we define the sum of mean arrival times at  $\bar{x}_j$  of all vehicles present in  $I_j$  within the time interval  $[0, T]$  as

$$\mathcal{M}_{T, \bar{x}}(A, \gamma; \bar{u}) \doteq \sum_{j \in \mathcal{O}} \frac{\int_0^T t f_j(u_j(t, \bar{x}_j; A, \gamma)) dt}{\int_0^{\tau_j} \sum_{i \in \mathcal{I}} a_{ji}(t) \gamma_i(t) dt + \int_0^{\bar{x}_j} \bar{u}_j(x) dx}. \quad (13)$$

**Queue length.** The length of traffic queues forming upstream of bottlenecks or of red lights located at  $\bar{x}_j$ ,  $j \in \mathcal{O}$ , can be measured as in [19] by introducing nondecreasing, Lipschitz continuous, weight maps  $\Psi_j: \Omega_j \rightarrow [0, 1]$ , that value 0 whenever the vehicular density is below 75% of the maximum density  $u_j^{max}$ , while value 1 whenever the vehicular density is above 85% of  $u_j^{max}$ . Then, for every  $(A, \gamma) \in \mathcal{U}$ , we define the functional

$$\mathcal{Q}_{T, \bar{x}}(A, \gamma; \bar{u}) \doteq \sum_{j \in \mathcal{O}} \int_0^T \int_{\bar{x}_j - \rho_j}^{\bar{x}_j} \Psi_j(u_j(t, x; A, \gamma)) dx dt, \quad (14)$$

for some constant  $0 < \rho_j < \bar{x}_j$ ,  $j \in \mathcal{O}$ .

**Stop-and-go waves.** Instabilities of traffic flow as density increases are caused by the delays in adapting the vehicular speed to the actual traffic conditions, due to finite accelerations and reaction times of human drivers. These small perturbations determine the formation of stop-and-go-waves that travel backward along the road (e.g. see [22, 32, 33, 46, 49]). A golden rule of traffic flow optimization is try to homogenize traffic flow with respect to time and space so to reduce probability of accidents and pollution [50]. Thus, a relevant criterion in the traffic management is the minimization of stop-and-go-waves [28, 45, 48]. From the mathematical point of view this corresponds to minimise the total variation of the traffic density or speed. Following [17] we then introduce lower semicontinuous weight maps  $p_j: I_j \rightarrow [0, 1]$ ,  $j \in \mathcal{O}$ , taking higher values in more dangerous sections of  $I_j$ , and, for every  $(A, \gamma) \in \mathcal{U}$ , we define

$$\mathcal{J}_{T, \bar{x}}(A, \gamma; \bar{u}) \doteq \sum_{j \in \mathcal{O}} \int_0^T \int_0^{\bar{x}_j} p_j(x) d|\partial_x u_j(t, x; A, \gamma)| dt, \tag{15}$$

where we are integrating  $p_j$  with respect to the total variation measure  $|\partial_x u_j(t, x)|$ .

**Fuel consumption.** Vehicle fuel consumption and emissions are two critical aspects considered by transportation planners. As for the travel time concept, various definition to quantify the overall fuel consumption have been introduced in the literature based on microscopic and macroscopic models (see [1, 50]). We consider here the definition proposed in [43] (see also [42]), where the fuel consumption rate in a macroscopic model is expressed by a function depending on the average traffic speed. Taking into account the experimental evidence that the consumption per distance increases when travelling at very low speeds (a certain amount of fuel is anyway used to just keep the engine running) or at very high speeds (more energy is needed to overcome air resistance), we thus introduce a Lipschitz continuous function  $K_j(v)$ , which is decreasing in a right neighbourhood of 0 and increasing in a left neighbourhood of  $v_j^{max} \doteq \max_{u \in \Omega_j} v_j(u)$ ,  $j \in \mathcal{O}$  ( $v_j$  being the speed of Assumption (A) in Section 2). Then, for every  $(A, \gamma) \in \mathcal{U}$ , we define

$$\mathcal{F}_{T, \bar{x}}(A, \gamma; \bar{u}) \doteq \sum_{j \in \mathcal{O}} \int_0^T \int_0^{\bar{x}_j} u_j(t, x; A, \gamma) K_j(v_j(u_j(t, x; A, \gamma))) dx dt. \tag{16}$$

### 5. Existence of optimal solutions

We start proving the semicontinuity and continuity of the previous functionals with respect to  $\mathbf{L}^1$  convergence.

**Proposition 5.1.** *Fix  $\bar{u} \in \Pi_{\ell=1}^{m+n} \mathbf{L}^\infty(I_\ell; \Omega_\ell)$ . Then, for every  $T > 0$ ,  $\bar{x} \in \Pi_{j=m+1}^{m+n} I_j$ , the functionals (11), (13), (15) are sequentially lower semicontinuous and the functionals (14), (16) are continuous with respect to the  $\mathbf{L}^1_{loc}$  convergence on the set  $\mathcal{U}^M$  defined in (10), for every  $M > 0$ .*

**Proof.** The proof is divided into several steps.

1. Consider a sequence  $((A^\nu, \gamma^\nu))_\nu$  in  $\mathcal{U}^M$ ,  $A^\nu = (a_{ji}^\nu)_{ji}$ , such that

$$\begin{aligned} A^\nu &\rightarrow A && \text{in } \mathbf{L}^1((0, T); \mathbb{R}^{m \times n}), \\ \gamma^\nu &\rightarrow \gamma && \text{in } \mathbf{L}^1((0, T); \mathbb{R}^m), \end{aligned} \quad \text{as } \nu \rightarrow \infty, \tag{17}$$

for some  $(A, \gamma) \in \mathcal{U}^M$ ,  $A = (a_{ji})_{ji}$ .

Observe that, setting

$$\begin{aligned} u_\ell^\nu(t, x) &\doteq u_\ell^\nu(t, x; A^\nu, \gamma^\nu), & u_\ell(t, x) &\doteq u_\ell(t, x; A, \gamma) & \ell \in \mathcal{I} \cup \mathcal{O}, \\ \gamma_j^\nu(t) &\doteq \sum_{i=1}^m a_{ji}^\nu(t) \gamma_i^\nu(t), & \gamma_j(t) &\doteq \sum_{i=1}^m a_{ji}(t) \gamma_i(t) & j \in \mathcal{O}, \end{aligned} \tag{18}$$

and recalling Definition 3.1, we have

$$f_\ell(u_\ell^\nu(t, 0)) = \gamma_\ell^\nu(t), \quad f_\ell(u_\ell(t, 0)) = \gamma_\ell(t) \quad \forall t > 0, \ell \in \mathcal{I} \cup \mathcal{O}. \tag{19}$$

Hence, since  $(\gamma_\ell^\nu)_\nu$  take values in the bounded set  $f_\ell(\Omega_\ell)$ , for all  $\ell \in \mathcal{I} \cup \mathcal{O}$ , and  $(a_{ji}^\nu)_\nu$  are uniformly bounded because of (9), (10), relying on (17) we deduce that

$$f_\ell(u_\ell^\nu(\cdot, 0)) \rightarrow f_\ell(u_\ell(\cdot, 0)) \quad \text{in} \quad \mathbf{L}^1((0, T); \mathbb{R}) \quad \forall \ell \in \mathcal{I} \cup \mathcal{O}. \tag{20}$$

Then, by virtue of the  $\mathbf{L}^1$  Lipschitz continuous dependence of the solution to (4) on the initial data and on the boundary-flux (see Remark 2.3), we deduce from (20) that, for all  $j \in \mathcal{O}$ , there holds

$$u_j^\nu(t, \cdot) \rightarrow u_j(t, \cdot) \quad \text{in} \quad \mathbf{L}^1([0, +\infty); \Omega_j) \quad \forall t \in [0, T], \tag{21}$$

and

$$\iint_{[0, T] \times [0, +\infty)} \left| u_j^\nu(t, x) - u_j(t, x) \right| dx dt \leq T \int_0^T \left| f_j(u_j^\nu(t, 0)) - f_j(u_j(t, 0)) \right| dt. \tag{22}$$

In turn, (22) together with (20), yields

$$u_j^\nu \rightarrow u_j \quad \text{in} \quad \mathbf{L}^1([0, T] \times [0, +\infty); \Omega_j) \quad \forall j \in \mathcal{O}. \tag{23}$$

**2.** Relying on (20), (23), we shall now obtain the convergence of the functionals (11)–(16) evaluated at  $(A^\nu, \gamma^\nu)$ .

Since  $(u_j^\nu)_\nu$  take values in the bounded set  $\Omega_j$ , and  $\Psi_j, K_j, v_j$  are Lipschitz continuous maps, it is immediate to see that (23) implies  $\mathcal{Q}_{T, \bar{x}}(A, \gamma; \bar{u}) = \lim_{\nu \rightarrow \infty} \mathcal{Q}_{T, \bar{x}}(A^\nu, \gamma^\nu; \bar{u})$  and  $\mathcal{F}_{T, \bar{x}}(A, \gamma; \bar{u}) = \lim_{\nu \rightarrow \infty} \mathcal{F}_{T, \bar{x}}(A^\nu, \gamma^\nu; \bar{u})$ , which proves the continuity of the functionals (14), (16).

Next, observe that, relying on (21), with the same arguments in [17] we derive  $\mathcal{J}_{T, \bar{x}}(A, \gamma; \bar{u}) \leq \liminf_{\nu \rightarrow \infty} \mathcal{J}_{T, \bar{x}}(A^\nu, \gamma^\nu; \bar{u})$ , proving the sequential lower semicontinuity of the functional (15).

As to the functional in (13), recall that by Definition 2.2(i) we have  $u_j(t) \in \mathbf{BV}_{\text{loc}}(I_j)$  for all  $t > 0$ . Then, applying a general property of BV weak solutions of conservation laws (e.g. see [3, Proposition 2.1]), we deduce that for all  $t \in (0, T)$  we have for all  $\nu$

$$\begin{aligned} \int_t^T f_j(u_j(s, \bar{x}_j)) ds &= \int_t^T f_j(u_j(s, 0)) ds + \int_0^{\bar{x}_j} u_j(t, x) dx - \int_0^{\bar{x}_j} u_j(T, x) dx, \\ \int_t^T f_j(u_j^\nu(s, \bar{x}_j)) ds &= \int_t^T f_j(u_j^\nu(s, 0)) ds + \int_0^{\bar{x}_j} u_j^\nu(t, x) dx - \int_0^{\bar{x}_j} u_j^\nu(T, x) dx. \end{aligned} \tag{24}$$

Because of (20)–(21), we derive from (24) that

$$f_j(u_\ell^\nu(\cdot, \bar{x}_j)) \rightarrow f_j(u_j(\cdot, \bar{x}_j)) \text{ in } \mathbf{L}^1((0, T); \mathbb{R}) \quad \forall j \in \mathcal{O}. \quad (25)$$

Notice that, by (12), (18), there will be  $(\tau_j^\nu)_\nu \subset [0, T]$  such that

$$\int_0^T f_j(u_j^\nu(t, \bar{x}_j)) dt = \int_0^{\tau_j^\nu} \gamma_j^\nu(t) dt + \int_0^{\bar{x}_j} \bar{u}_j(x) dx \quad \forall j \in \mathcal{O}, \quad \forall \nu.$$

By compactness, we may assume for any  $j \in \mathcal{O}$  that, up to a subsequence, one has  $\tau_j^\nu \rightarrow \tau_j$ , for some  $\tau_j \in [0, T]$ . Thus, thanks to (19), (20), (25), we find

$$\int_0^T f_j(u_j(t, \bar{x}_j)) dt = \int_0^{\tau_j} \gamma_j(t) dt + \int_0^{\bar{x}_j} \bar{u}_j(x) dx \quad \forall j \in \mathcal{O}.$$

Then, recalling (13), (18), we write

$$\begin{aligned} \mathcal{M}_{T, \bar{x}}(A^\nu, \gamma^\nu; \bar{u}) &= \sum_{j \in \mathcal{O}} \frac{\int_0^T t f_j(u_j^\nu(t, \bar{x}_j)) dt}{\int_0^{\tau_j^\nu} \gamma_j^\nu(t) dt + \int_0^{\bar{x}_j} \bar{u}_j(x) dx}, \\ \mathcal{M}_{T, \bar{x}}(A, \gamma; \bar{u}) &= \sum_{j \in \mathcal{O}} \frac{\int_0^T t f_j(u_j(t, \bar{x}_j)) dt}{\int_0^{\tau_j} \gamma_j(t) dt + \int_0^{\bar{x}_j} \bar{u}_j(x) dx}. \end{aligned}$$

Hence, for every fixed  $\delta > 0$ , relying on (19), (20), (25), using the dominated convergence theorem and the property of  $\liminf$ , we get that, up to a subsequence, we have

$$\begin{aligned} \liminf_{\nu \rightarrow \infty} \mathcal{M}_{T, \bar{x}}(A^\nu, \gamma^\nu; \bar{u}) &\geq \sum_{j \in \mathcal{O}} \liminf_{\nu \rightarrow \infty} \frac{\int_0^T t f_j(u_j^\nu(t, \bar{x}_j)) dt}{\int_0^{\tau_j^\nu} \gamma_j^\nu(t) dt + \int_0^{\bar{x}_j} \bar{u}_j(x) dx} \\ &\geq \sum_{j \in \mathcal{O}} \lim_{\nu \rightarrow \infty} \frac{\int_0^T t f_j(u_j^\nu(t, \bar{x}_j)) dt}{\int_0^{\tau_j^\nu} \gamma_j^\nu(t) dt + \int_0^{\bar{x}_j} \bar{u}_j(x) dx} + \delta = \sum_{j \in \mathcal{O}} \frac{\int_0^T t f_j(u_j(t, \bar{x}_j)) dt}{\int_0^{\tau_j} \gamma_j(t) dt + \int_0^{\bar{x}_j} \bar{u}_j(x) dx} + \delta. \end{aligned} \quad (26)$$

Sending  $\delta \rightarrow 0$  in (26) we deduce

$$\mathcal{M}_{T, \bar{x}}(A, \gamma; \bar{u}) \leq \liminf_{\nu \rightarrow \infty} \mathcal{M}_{T, \bar{x}}(A^\nu, \gamma^\nu; \bar{u}),$$

proving the sequential lower semicontinuity of the functional (13).

Finally, we can show the semicontinuity of the functional (11) by the same arguments used for the functional (13). Namely, fix  $\delta > 0$ . Then, relying on (18), (23), on the continuity of the maps  $v_j$  and on the property of  $\liminf$ , and using the dominated convergence theorem, we get that, up to a subsequence, we have

$$\begin{aligned} \liminf_{\nu \rightarrow \infty} \mathcal{T}_{T, \bar{x}}(A^\nu, \gamma^\nu; \bar{u}) &\geq \frac{1}{T} \sum_{j \in \mathcal{O}} \liminf_{\nu \rightarrow \infty} \int_0^T \int_0^{\bar{x}_j} \frac{1}{v_j(u_j^\nu(t, x))} dx dt \\ &\geq \frac{1}{T} \sum_{j \in \mathcal{O}} \lim_{\nu \rightarrow \infty} \int_0^T \int_0^{\bar{x}_j} \frac{1}{v_j(u_j^\nu(t, x)) + \delta} dx dt = \frac{1}{T} \sum_{j \in \mathcal{O}} \int_0^T \int_0^{\bar{x}_j} \frac{1}{v_j(u_j(t, x)) + \delta} dx dt. \end{aligned} \quad (27)$$

Letting  $\delta \rightarrow 0$  in (27) and using the monotone convergence theorem, we deduce  $\mathcal{T}_{T, \bar{x}}(A, \gamma; \bar{u}) \leq \liminf_{\nu \rightarrow \infty} \mathcal{T}_{T, \bar{x}}(A^\nu, \gamma^\nu; \bar{u})$ , which shows the sequential lower semi-continuity of the functional (11) and concludes the proof.  $\square$

**Corollary 5.2.** Fix  $T > 0$ ,  $\bar{x} \in \Pi_{j=m+1}^{m+n} I_j$ , and  $\bar{u} \in \Pi_{\ell=1}^{m+n} \mathbf{L}^\infty(I_\ell; \Omega)$ . Then, for every  $M > 0$ , the functionals (11), (13), (14), (15), (16) admit a minimum on the set  $\mathcal{U}^M$  defined in (10). Moreover, if  $\bar{u}_j(x) \in [0, \theta_j]$  for every  $j \in \mathcal{O}$  and a.e.  $x > 0$ , then for every  $M > 0$ ,  $0 < K \leq 1$ , the functionals (11), (13), (14), (15), (16) admit a minimum on the set  $\mathcal{U}_K^M$  defined in (10).

**Proof.** The fact that the various functionals admit a minimum on  $\mathcal{U}^M$  follows from Proposition 5.1 and from Theorem 3.3. The latter statement follows similarly using also Remark 3.2.  $\square$

### 6. Equivalent variational formulations

We present here an equivalent variational formulation of the optimization problem on the set  $\mathcal{U}_K^M$  for the functionals defined in Section 4, which may be useful also for numerical investigations. Namely, for every fixed  $T > 0$ ,  $M > 0$  and  $0 < K \leq 1$ , consider the function

$$I(\delta) = \min_{(A, \gamma) \in \mathcal{U}^M(\bar{u})} \left\{ \mathcal{J}_1(A, \gamma; \bar{u}) + \frac{1}{\delta} \sum_{i \in \mathcal{I}} \left( K \bar{c}_i^T - \int_0^T \gamma_i(t) dt \right)^+ \right\} \quad (28)$$

where  $\mathcal{J}_1$  is any of the functionals (11), (13), (14), (15), (16), and  $(\cdot)^+$  denotes the positive part. Since the function

$$(A, \gamma) \mapsto \sum_{i \in \mathcal{I}} \left( K \bar{c}_i^T - \int_0^T \gamma_i(t) dt \right)^+$$

is continuous in the  $\mathbf{L}^1$  topology, the minimum in (28) is well defined.

**Theorem 6.1.** Given  $\bar{u} \in \Pi_{\ell=1}^{m+n} \mathbf{L}^\infty(I_\ell; \Omega)$ , and  $T > 0$ , for every fixed  $M > 0$  one has

$$\lim_{\delta \rightarrow 0^+} I(\delta) = \min_{(A, \gamma) \in \mathcal{U}_K^M(\bar{u})} \mathcal{J}_1(A, \gamma; \bar{u}). \quad (29)$$

**Proof.** For  $\delta > 0$ , define  $(A^\delta, \gamma^\delta) \in \mathcal{U}^M$  a point of minimum for (28). By Theorem 3.3 the set  $\mathcal{U}^M$  is compact; hence there exists  $(A^*, \gamma^*) \in \mathcal{U}^M(\bar{u})$  such that, up to a subsequence,

$$(A^\delta, \gamma^\delta) \longrightarrow (A^*, \gamma^*)$$

in the  $\mathbf{L}^1$ -topology for  $\delta \rightarrow 0^+$ . By the minimality of  $(A^\delta, \gamma^\delta)$  we deduce that

$$\mathcal{J}_1(A^\delta, \gamma^\delta; \bar{u}) + \frac{1}{\delta} \sum_{i \in \mathcal{I}} \left( K \bar{c}_i^T - \int_0^T \gamma_i^\delta(t) dt \right)^+ \leq \min_{(A, \gamma) \in \mathcal{U}_K^M(\bar{u})} \{ \mathcal{J}_1(A, \gamma; \bar{u}) \}$$

and so, by lower semicontinuity of  $\mathcal{J}_1$ , we obtain that

$$\liminf_{\delta \rightarrow 0^+} -\frac{1}{\delta} \sum_{i \in \mathcal{I}} \left( K \bar{c}_i^T - \int_0^T \gamma_i^\delta(t) dt \right)^+ \geq \mathcal{J}_1(A^*, \gamma^*; \bar{u}) - \min_{(A, \gamma) \in \mathcal{U}_K^M(\bar{u})} \{ \mathcal{J}_1(A, \gamma; \bar{u}) \}. \quad (30)$$

Since the positive part is continuous with respect to the  $\mathbf{L}^1$  topology, we have that

$$\lim_{\delta \rightarrow 0^+} \sum_{i \in \mathcal{I}} \left( K \bar{c}_i^T - \int_0^T \gamma_i^\delta(t) dt \right)^+ = \sum_{i \in \mathcal{I}} \left( K \bar{c}_i^T - \int_0^T \gamma_i^*(t) dt \right)^+ \geq 0.$$

If  $\sum_{i \in \mathcal{I}} \left( K \bar{c}_i^T - \int_0^T \gamma_i^*(t) dt \right)^+ > 0$ , then

$$\liminf_{\delta \rightarrow 0^+} -\frac{1}{\delta} \sum_{i \in \mathcal{I}} \left( K \bar{c}_i^T - \int_0^T \gamma_i^\delta(t) dt \right)^+ = -\infty,$$

which is a contradiction to (30). Therefore

$$\sum_{i \in \mathcal{I}} \left( K \bar{c}_i^T - \int_0^T \gamma_i^*(t) dt \right)^+ = 0,$$

which implies that  $(A^*, \gamma^*) \in \mathcal{U}_M^K(\bar{u})$ . Moreover (30) implies also that

$$\mathcal{J}_1(A^*, \gamma^*; \bar{u}) \leq \min_{(A, \gamma) \in \mathcal{U}_K^M(\bar{u})} \{ \mathcal{J}_1(A, \gamma; \bar{u}) \}$$

proving that  $(A^*, \gamma^*)$  is the point of minimum for  $\mathcal{J}_1$  on  $\mathcal{U}_M^K(\bar{u})$ .

This concludes the proof. □

### 7. Numerical simulations

In this section we present few numerical simulations in the case of a node with two incoming and two outgoing arcs; see Figure 7.1. Similar to the numerical results in [3], the optimal solutions related to traffic indexes of Section 4 seem to be different from the solution obtained through a Riemann Solver at the junction; see [23]. Starting from two different sets of initial conditions, we make a comparison between the solution obtained with the Riemann Solver at the junction (see for more details [14, 23]) and the solution obtained considering the functionals of Section 4. Since the network topology is very simple and the outgoing roads are not congested, we do not consider the *queue length* functional (14), since in this situation it is constantly equal to 0.

In the examples of this section, we describe the incoming roads  $I_1$  and  $I_2$  and the outgoing ones  $I_3$  and  $I_4$  respectively through the real intervals  $(-15, 0)$  and  $(0, 15)$ .

In each arc, the PDE (1) is considered together with the flux function given by  $f_\ell(u) = 4u(1 - u)$ , so that the set  $\Omega_\ell$  of all the possible densities is the interval  $[0, 1]$ .

The numerical solution in each arc is computed through the Godunov method, which is based on the solution to Riemann problems; see for example [38, Section 12.1]

or [30, Chapter 3]. We use a uniform spatial mesh with length  $\Delta x = 0.05$  and a non-uniform time mesh with length  $\Delta t$ , calculated in such a way the classic CFL condition is satisfied; see [38, Section 4.4] or [47, Definition 5.1]. The simulations are done in the time interval  $(0, T)$ .

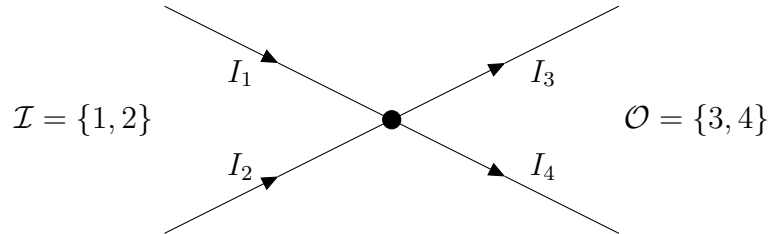


Figure 7.1: The junction considered in Section 7. The incoming roads are denoted by  $I_1$  and  $I_2$ , while the outgoing ones are denoted by  $I_3$  and  $I_4$ .

Concerning the optimization problem, we first assume that the distributional matrix  $A$  satisfying (7) is a priori fixed: we only regard as junction controls the incoming fluxes  $\gamma = (\gamma_1, \gamma_2)$ . Moreover, according to Theorem 6.1, we choose to minimize the variational functional defined in (28), with the parameters  $\delta = 0.003$ ,  $\bar{x}_3 = \bar{x}_4 = 5$ , and  $K = 0.9$ . In order to numerically approximate an optimal control for minimizing (28), we perform a gradient descent or steepest descent method; see [8]. This is a first order iterative method for finding local minima or maxima of a functional  $\mathcal{I}$ . More precisely, given a control  $\gamma^0$ , we calculate the approximate gradient  $\nabla \mathcal{I}(\gamma^0)$ , and we construct another control  $\gamma^1$  such that the difference  $\gamma^1 - \gamma^0$  is proportional to  $\nabla \mathcal{I}(\gamma^0)$ . In the simulations, we assume that the control is a piecewise constant function with (at most) 200 points of discontinuity equally spaced.

### 7.1. First example

	Optimal cost	Riemann Solver
Average travel time	3.03	3.46
Mean arrival time	9.33	9.40
Stop-and-go waves	0.06	0.16
Fuel consumption	19.74	25.98

Table 7.1: The values of the functionals of Section 4 related to the parameters contained in Subsection 7.1. In the column “Optimal cost” the values of the *optimal* solution, obtained with the gradient descent method. In the column “Riemann Solver”, the values of the various functionals for the solution obtained with the junction Riemann Solver.

We consider a situation where, initially, the outgoing roads are empty, one incoming road is congested and one not. More precisely, we have the following initial data:

$$\bar{u}_1(x) = 0.3\chi_{(-14,0)}(x), \quad \bar{u}_2(x) = 0.5\chi_{(-14,-4)}(x) + 0.7\chi_{(-4,0)}(x), \quad \bar{u}_3(x) = \bar{u}_4(x) = 0.$$

We consider the distribution matrix  $A = \begin{pmatrix} 0.75 & 0.6 \\ 0.25 & 0.4 \end{pmatrix}$ , which means that  $\frac{3}{4}$  cars in

$I_1$  wants to go in  $I_3$  and  $\frac{3}{5}$  cars in  $I_2$  wants to go in  $I_3$ . The simulation is performed until time  $T = 10$ . The solution obtained with the classical Riemann Solver at the junction is plotted in Figure 7.2. The values of the functionals of Section 4 evaluated for such solution are in Table 7.1.

The optimal solutions for the functionals of Section 4 are plotted in Figures 7.3, 7.4, 7.5, and 7.6.

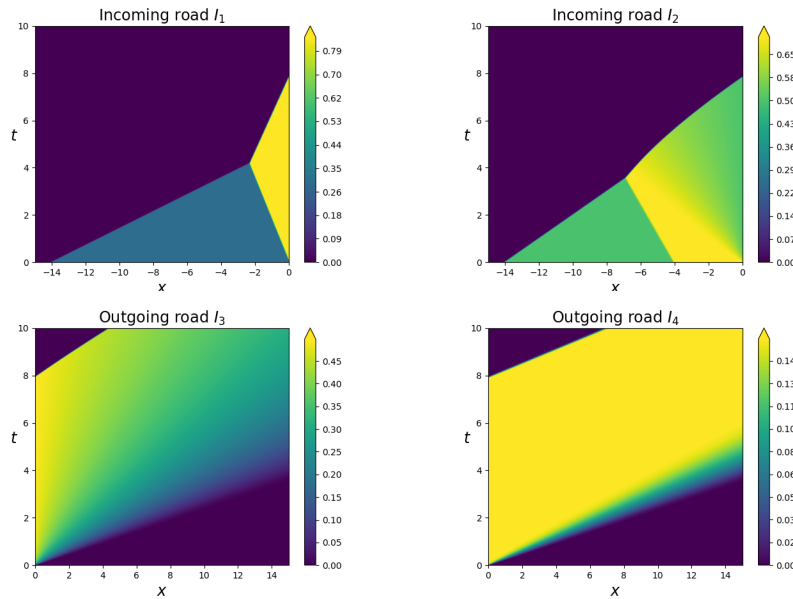


Figure 7.2: The contour plot of the solution obtained with the classical Riemann Solver at the node of the example of Subsection 7.1.

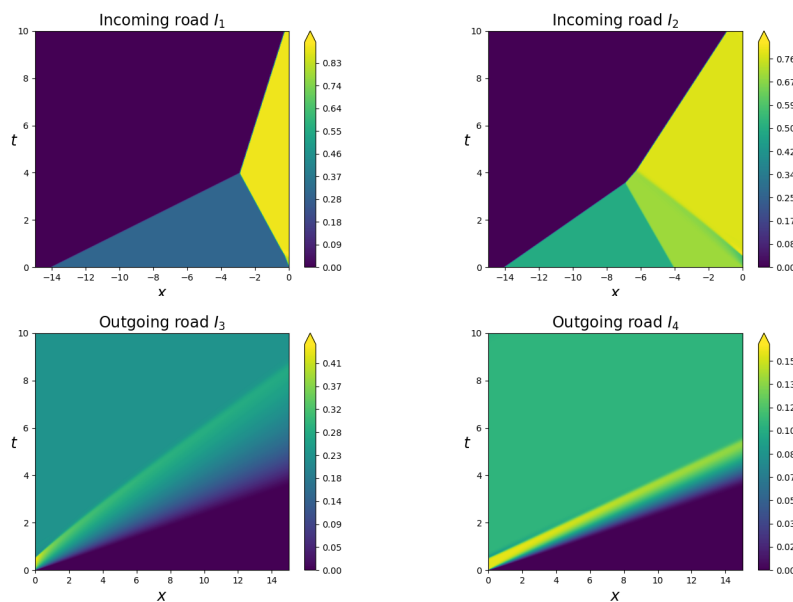


Figure 7.3: The contour plot for the solution obtained optimizing the functional *average travel time*, see (11), related to Subsection 7.1.

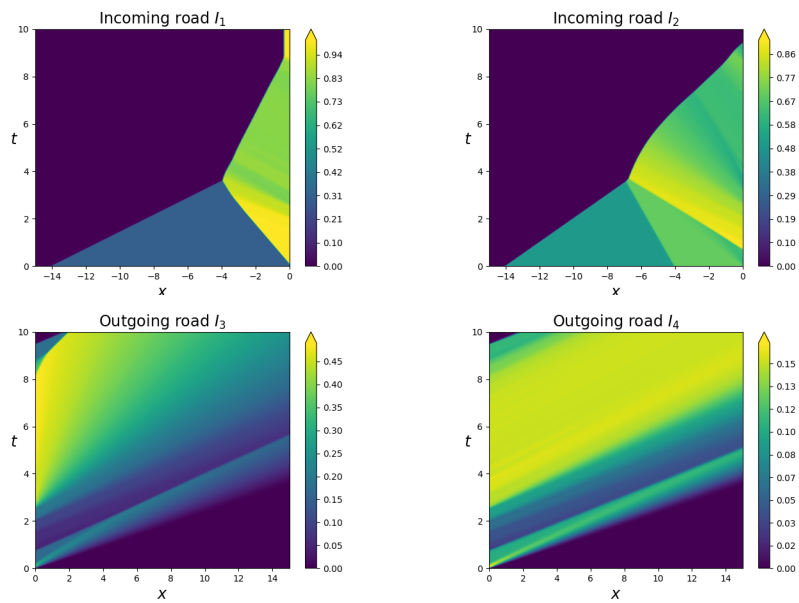


Figure 7.4: The contour plot for the solution obtained optimizing the functional *mean arrival time*, see (13), related to Subsection 7.1.

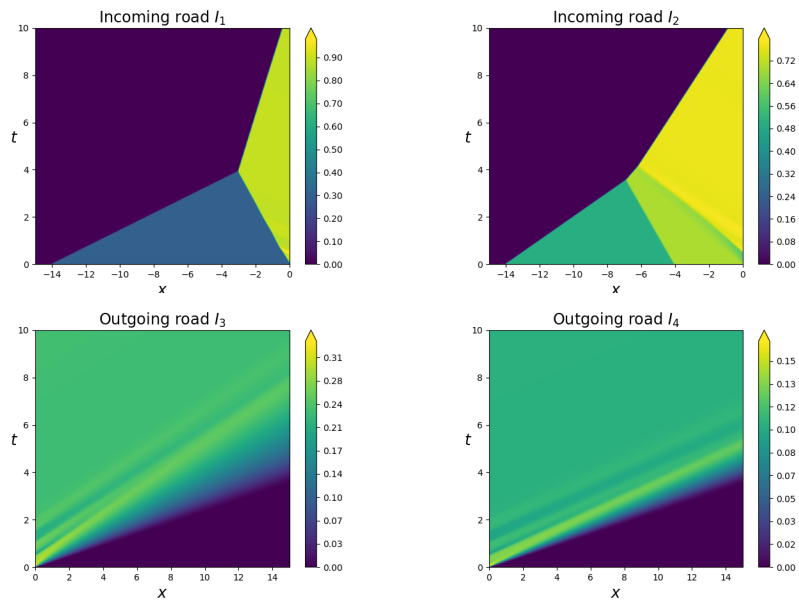


Figure 7.5: The contour plot for the solution obtained optimizing the functional *stop-and-go waves*, see (15), related to Subsection 7.1.

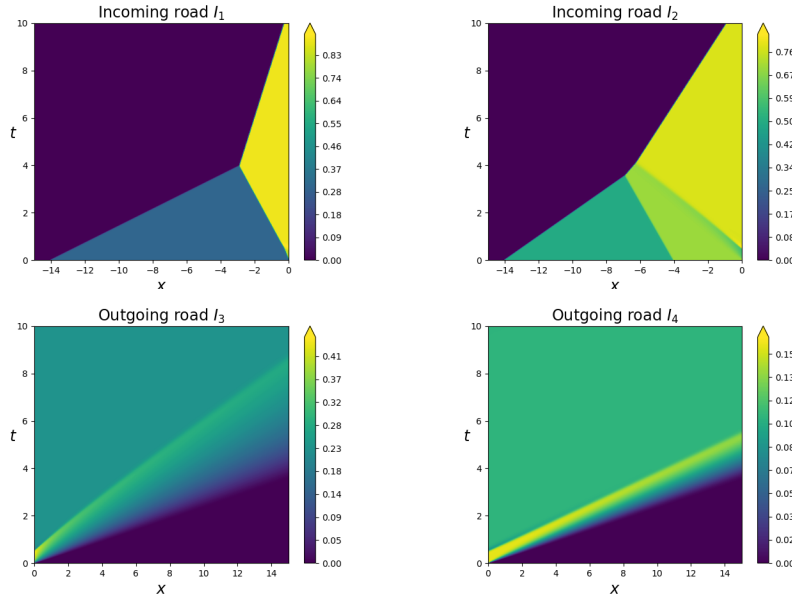


Figure 7.6: The contour plot for the solution obtained optimizing the functional *fuel consumption*, see (16), related to Subsection 7.1.

### 7.2. Second example

Let us consider a situation where, initially, the outgoing roads are empty and the incoming roads are equally crowded. More precisely we deal with the following initial data:

$$\bar{u}_1(x) = \bar{u}_2(x) = 0.5\chi_{(-14,-4)}(x) + 0.7\chi_{(-4,0)}(x), \quad \bar{u}_3(x) = \bar{u}_4(x) = 0.$$

We consider the following distribution matrix

$$A = \begin{pmatrix} 0.75 & 0.6 \\ 0.25 & 0.4 \end{pmatrix},$$

which means that  $\frac{3}{4}$  cars in  $I_1$  wants to go in  $I_3$  and  $\frac{3}{5}$  cars in  $I_2$  wants to go in  $I_3$ . The simulation is performed until time  $T = 10$ . The solution obtained with the classical Riemann Solver at the junction is plotted in Figure 7.7. The values of the functionals of Section 4 evaluated for such solution are in Table 7.2. Note that the solution generated by the junction Riemann Solver does not respect the constraint

$$\sum_{i \in \mathcal{I}} \left( K \bar{c}_i^T - \int_0^T \gamma_i(t) dt \right)^+ = 0.$$

In particular, from  $I_1$ , during the time interval  $(0, T)$ , the number of cars passing through the junction is less than the 90% of the value  $\bar{c}_1^T$ . In this situation the penalization term

$$\frac{1}{\delta} \sum_{i \in \mathcal{I}} \left( K \bar{c}_i^T - \int_0^T \gamma_i(t) dt \right)^+ = \frac{1}{\delta} \left( K \bar{c}_1^T - \int_0^T \gamma_1(t) dt \right)^+ \sim 246.46$$

is applied to the functionals.

The optimal solutions for the functionals of Section 4 are plotted in Figures 7.8, 7.9, 7.10, and 7.11.

	Optimal cost	R-S	R-S no penalization
<b>Average travel time</b>	3.42	250.00	3.55
Mean arrival time	9.37	255.83	9.37
Stop-and-go waves	0.07	246.59	0.13
Fuel consumption	26.91	274.90	28.44

Table 7.2: The values of the functionals of Section 4 related to the parameters contained in Subsection 7.2. In the column “Optimal cost” the values of the *optimal* solution, obtained with the gradient descent method. In the column “R-S”, the values of the various functionals for the solution obtained with the junction Riemann Solver. In the column “R-S no penalization”, the values of the various functionals without the penalization term, which is equal to 246.46, for the solution obtained with the junction Riemann Solver.

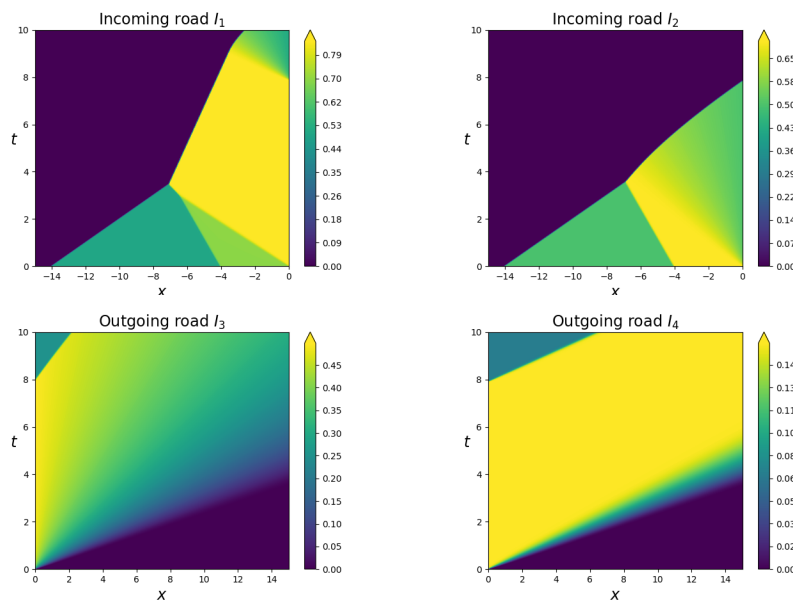
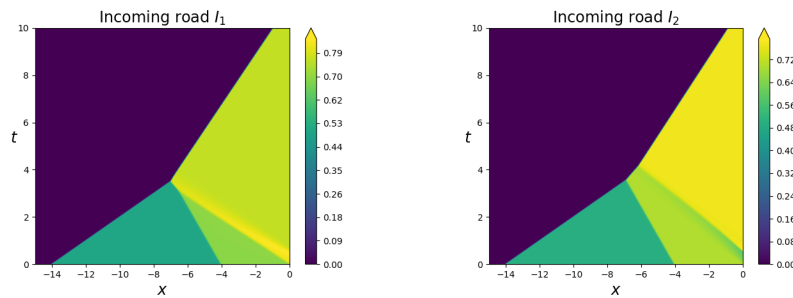


Figure 7.7: The contour plot of the solution obtained with the classical Riemann Solver at the node of the example of Subsection 7.2.



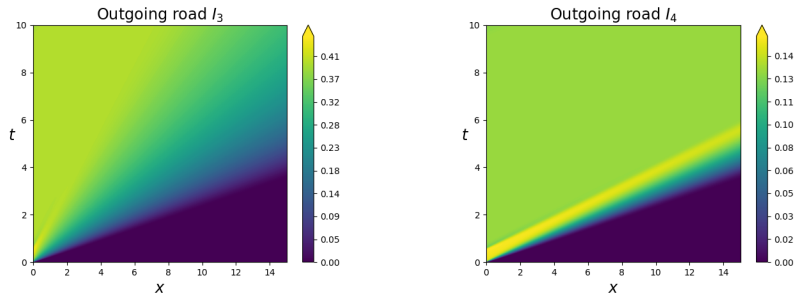


Figure 7.8: The contour plot for the solution obtained optimizing the functional *average travel time*, see (11), related to Subsection 7.2.

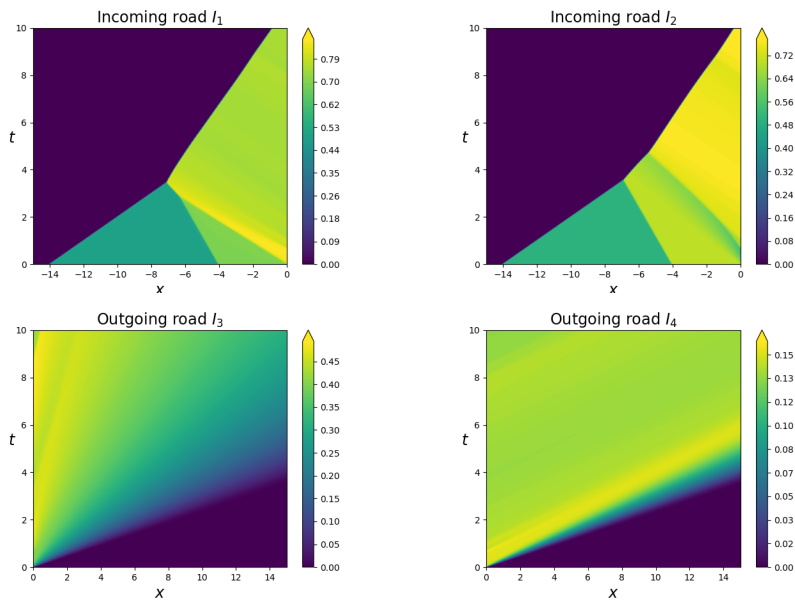


Figure 7.9: The contour plot for the solution obtained optimizing the functional *mean arrival time*, see (13), related to Subsection 7.2.

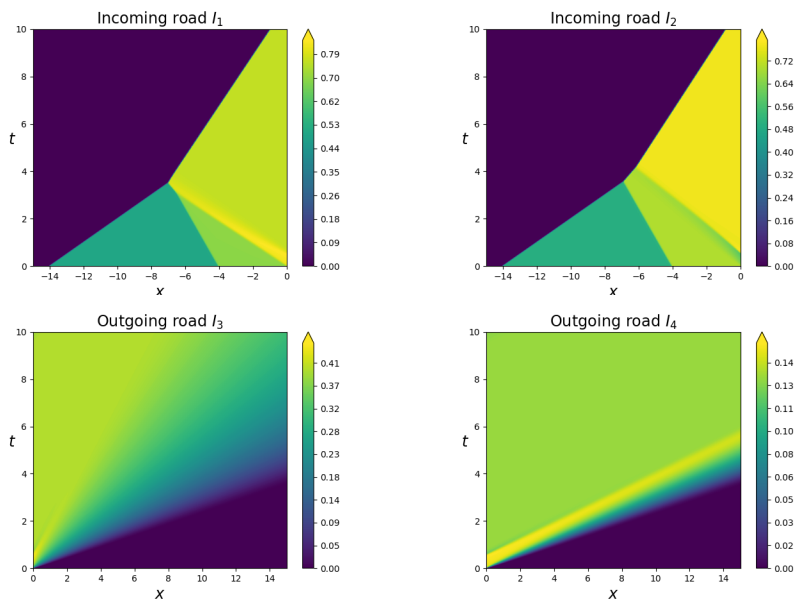


Figure 7.10: The contour plot for the solution obtained optimizing the functional *stop-and-go waves*, see (15), related to Subsection 7.2.

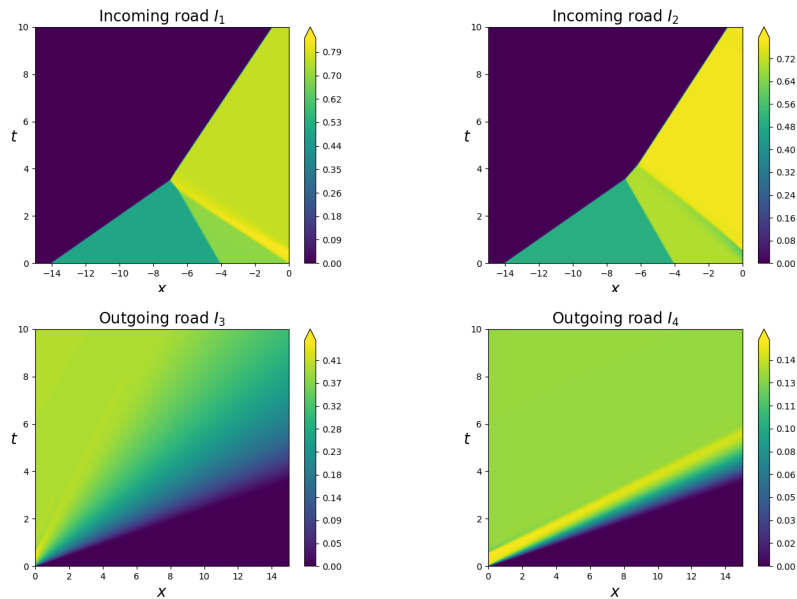


Figure 7.11: The contour plot for the solution obtained optimizing the functional fuel consumption, see (16), related to Subsection 7.2.

## References

- [1] K. Ahn, H. Rakha, A. Trani, M. Van Aerde: *Estimating vehicle fuel consumption and emissions based on instantaneous speed and acceleration levels*, J. Transportation Eng. 128(2) (2002) 182–190.
- [2] L. Ambrosio, N. Fusco, D. Pallara: *Functions of Bounded Variation and Free Discontinuity Problems*, Oxford Mathematical Monographs, Clarendon – Oxford University Press, New York (2000).
- [3] F. Ancona, A. Cesaroni, G. M. Coclite, M. Garavello: *On the optimization of conservation law models at a junction with inflow and flow distribution controls*, SIAM J. Control Optimization 56(5) (2018) 3370–3403.
- [4] F. Ancona, M. T. Chiri: *Attainable profiles for conservation laws with flux function spatially discontinuous at a single point*, ESAIM: COCV 26 (2020), art. no. 124.
- [5] F. Ancona, A. Marson: *On the attainable set for scalar nonlinear conservation laws with boundary control*, SIAM J. Control Optimization 36(1) (1998) 290–312.
- [6] F. Ancona, A. Marson: *Scalar non-linear conservation laws with integrable boundary data*, Nonlinear Analysis 35 (1999) 687–710.
- [7] C. Bardos, A. Y. Le Roux, J.-C. Nédélec: *First order quasilinear equations with boundary conditions*, Comm. Partial Diff. Equations 4(9) (1979) 1017–1034.
- [8] A. Beck: *First-Order Methods in Optimization*, MOS-SIAM Series on Optimization 25, SIAM, Philadelphia (2017).
- [9] A. Bressan, S. Canic, M. Garavello, M. Herty, B. Piccoli: *Flow on networks: recent results and perspectives*, EMS Surveys Math. Sci. 1 (2014) 47–111.
- [10] G. Bretti, R. Natalini, B. Piccoli: *Numerical approximations of a traffic flow model on networks*, Networks Heterogeneous Media 1 (2006) 57–84.
- [11] R. C. Cascaval, C. D’Apice, M. P. D’Arienzo, R. Manzo: *Flow optimization in vascular networks*, Math. Biosci. Eng. 14(3) (2017) 607–624.

- [12] A. Cascone, C. D'Apice, B. Piccoli, L. Rarità: *Optimization of traffic on road networks*, Math. Models Methods Appl. Sci. 17(10) (2007) 1587–1617.
- [13] A. Cascone, A. Marigo, B. Piccoli, L. Rarità: *Decentralized optimal routing for packets flow on data networks*, Discrete Contin. Dyn. Syst., Ser. B 13(1) (2010) 59–78.
- [14] G. M. Coclite, M. Garavello, B. Piccoli: *Traffic flow on a road network*, SIAM J. Math. Analysis 36(6) (2005) 1862–1886.
- [15] R. M. Colombo, M. Garavello: *Control of biological resources on graphs*, ESAIM Control Optim. Calc. Var. 23(3) (2017) 1073–1097.
- [16] R. M. Colombo, P. Goatin, M. D. Rosini: *On the modelling and management of traffic*, ESAIM Math. Model. Numer. Analysis 45 (2011) 853–872.
- [17] R. M. Colombo, A. Groli: *Minimising stop and go waves to optimise traffic flow*, Appl. Math. Lett. 17 (2004) 697–701.
- [18] R. M. Colombo, G. Guerra, M. Herty, V. Schleper: *Optimal control in networks of pipes and canal*, SIAM J. Control Optimization 48(3) (2009) 2032–2050.
- [19] R. M. Colombo, E. Rossi: *IBVPs for scalar conservation laws with time discontinuous fluxes*, Math. Methods Appl. Sci. 41(4) (2018) 1463–1479.
- [20] C. D'Apice, S. Göttlich, M. Herty, B. Piccoli: *Modeling, Simulation, and Optimization of Supply Chains: A Continuous Approach*, SIAM, Philadelphia, PA, 2010.
- [21] C. D'Apice, R. Manzo, B. Piccoli, *Optimal input flow for a PDE-ODE model of supply chains*, Commun. Math. Sci., 10 (2012), 1225–1240.
- [22] M. R. Flynn, A. R. Kasimov, J.-C. Nave, R. R. Rosales, B. Seibold: *Self-sustained nonlinear waves in traffic flow*, Phys. Rev. E 79 (5) (2009) 056113-1–13.
- [23] M. Garavello, K. Han, B. Piccoli: *Models for Vehicular Traffic on Networks*, AIMS Series on Applied Mathematics 9, American Institute of Mathematical Sciences, Springfield (2016).
- [24] M. Garavello, B. Piccoli: *Traffic Flow on Networks, Volume 1*, AIMS Series on Applied Mathematics, American Institute of Mathematical Sciences, Springfield (2006).
- [25] S. Göttlich, S. Kühn, J. P. Ohst, S. Ruzika: *Evacuation modeling: a case study on linear and nonlinear network flow models*, EURO J. Comput. Optim. 4(3-4) (2016) 219–239.
- [26] K. Han, T. L. Friesz, T. Yao: *A variational approach for continuous supply chain networks*, SIAM J. Control Optimization 52(1) (2014) 663–686.
- [27] F. M. Hante, G. Leugering, A. Martin, L. Schewe, M. Schmidt: *Challenges in optimal control problems for gas and fluid flow in networks of pipes and canals: from modeling to industrial application*, in: *Industrial Mathematics and Complex Systems*, Industrial and Applied Mathematics, Springer, Singapore (2017) 77–122.
- [28] A. Hegyi, B. De Schutter, J. Hellendoorn: *Optimal coordination of variable speed limits to suppress shock waves*, IEEE Trans. Intell. Transp. Systems 6(1) (2005) 102–112.
- [29] M. Herty, M. Rascle: *Coupling conditions for a class of second-order models for traffic flow*, SIAM J. Math. Analysis 38(2) (2007) 595–616.
- [30] H. Holden, N. H. Risebro: *Front Tracking for Hyperbolic Conservation Laws*, 2nd edition, Applied Mathematical Sciences 152, Springer, Berlin (2015).
- [31] H. Holden, N. H. Risebro: *A mathematical model of traffic flow on a network of unidirectional roads*, SIAM J. Math. Analysis 26(4) (1995) 999–1017.

- [32] B. S. Kerner: *The Physics of Traffic: Empirical Freeway Pattern Features, Engineering Applications, and Theory*, Springer, Berlin (2012).
- [33] B. S. Kerner, P. Konhäuser: *Cluster effect in initially homogeneous traffic flow*, Phys. Rev. E 48 (1993) R2335–R2338.
- [34] M. La Marca, D. Armbruster, M. Herty, C. Ringhofer: *Control of continuum models of production systems*, IEEE Trans. Automatic Control 55 (2010) 2511–2526.
- [35] J.-P. Lebacque, M. Khoshyaran: *First order macroscopic traffic flow models for networks in the context of dynamic assignment*, Transportation Planning and Applied Optimization 64, M. Patriksson and M. Labbe (eds.), Springer, Berlin (2002) 119–140.
- [36] P. G. Le Floch: *Explicit formula for scalar non-linear conservation laws with boundary condition*, Math. Methods Appl. Sci. 10 (1988) 265–287.
- [37] P. G. Le Floch: *Hyperbolic Systems of Conservation Laws. The Theory of Classical and Nonclassical Shock Waves*, Lectures in Mathematics at the ETH Zürich, Birkhäuser, Basel (2002).
- [38] R. J. LeVeque: *Finite Volume Methods for Hyperbolic Problems*, Cambridge Texts in Applied Mathematics, Cambridge University Press, Cambridge (2002).
- [39] M. Lighthill, G. Whitham: *On kinematic waves. II: A theory of traffic flow on long crowded roads*, Proc. Royal Soc. London, Series A 229 (1955) 317–345.
- [40] J. Málek, J. Nečas, M. Rokyta, M. Růžička: *Weak and Measure-Valued Solutions to Evolutionary PDEs*, Applied Mathematics and Mathematical Computation 13, Chapman & Hall, London (1996).
- [41] F. Otto: *Initial-boundary value problem for a scalar conservation law*, C. R. Acad. Sci. Paris, Sér I Math 322(8) (1996) 729–734.
- [42] G. Piacentini, P. Goatin, A. Ferrara: *Traffic control via moving bottleneck of coordinated vehicles*, IFAC-PapersOnLine, 51(9) (2018) 13–18.
- [43] R. A. Ramadan, B. Seibold: *Traffic Flow Control and Fuel Consumption Reduction via Moving Bottlenecks*, arXiv: 1702.07995 (2017).
- [44] P. I. Richards, *Shock waves on the highway*, Oper. Res. 4 (1956) 42–51.
- [45] R. E. Stern, S. Cui, M. L. Delle Monache, R. Bhadani, M. Bunting, M. Churchill, N. Hamilton, R. Haulcy, H. Pohlmann, F. Wu, B. Piccoli, B. Seibold, J. Sprinkle, D. B. Work: *Dissipation of stop-and-go waves via control of autonomous vehicles: Field experiments*, Transp. Res. Part C 89 (2018) 205–221.
- [46] Y. Sugiyama, M. Fukui, M. Kikuchi, K. Hasebe, A. Nakayama, K. Nishinari, S.-i. Tadaki, S. Yukawa: *Traffic jams without bottlenecks – experimental evidence for the physical mechanism of the formation of a jam*, New J. Phys. 10(3) (2008) 033001 (7pp).
- [47] J. W. Thomas: *Numerical Partial Differential Equations: Finite Difference Methods*, Texts in Applied Mathematics 22, Springer, New York (1995).
- [48] E. Tomer, L. Safonov, N. Madar, S. Havlin: *Optimization of congested traffic by controlling stop-and-go waves*, Phys. Rev. E (3) 65(6) (2002) 065101, 4 pp.
- [49] M. Treiber, A. Hennecke, D. Helbing: *Congested traffic states in empirical observations and microscopic simulation*, Phys. Rev. E 62 (2000) 1805–1824.
- [50] M. Treiber, A. Kesting: *Traffic Flow Dynamics. Data, Models and Simulation*, Springer, Berlin (2013).